CHAPTER IV
RESULTS AND DISCUSSION

4.1 Emulsion stability

4.1.1 The influence of concentration of Pluronic f68 on the emulsion stability

Figure 4.1 shows a photograph of the emulsion stability after storage at room temperature (25 °C) for 24 hrs of 4% w/v silk fibroin and 15.33% w/v coconut at different concentration of Pluronic f68 that was used as surfactant. The thickness of the emulsion layer increased as the Pluronic f68 concentration increased and at 18.9% w/v Pluronic f68, there is a complete emulsion layer.

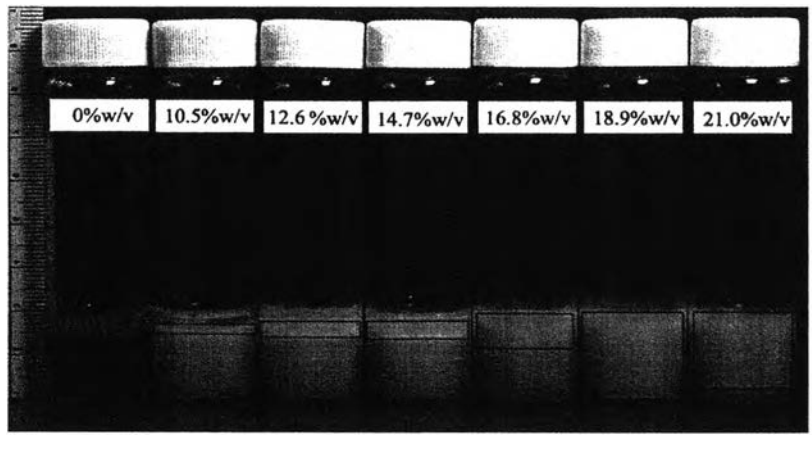

Figure 4.1 Photograph of the emulsion stability after 24 hrs of 15.33 % w/v coconut oil and 4% w/v silk at different concentrations of Pluronic f68 at solution volume ratio of Pluronic f68.

4.1.2 The influence of concentration of coconut oil on the emulsion stability

Figure 4.2 shows a photograph of the emulsions containing 18.9% w/v Pluronic f68 and 4% w/v silk fibroin at different concentration of coconut oil after storage at room temperature (25 °C) for 24 hrs. Increasing concentration of

coconut oil did not influenced to emulsion stability until 46% w/v coconut oil, there was a complete separation of emulsion into an oil layer at top layer. Observation of the emulsion that was stained with oil soluble dye (SudanIII)(Fig4.3A) and water soluble dye (Phenol red)(Fig4.3B) confirmed that the emulsion was oil in water type until 46% w/v coconut oil, there was water in oil emulsion because coconut oil excess to 18.9% w/v Pluronic f68 can stabilize it.

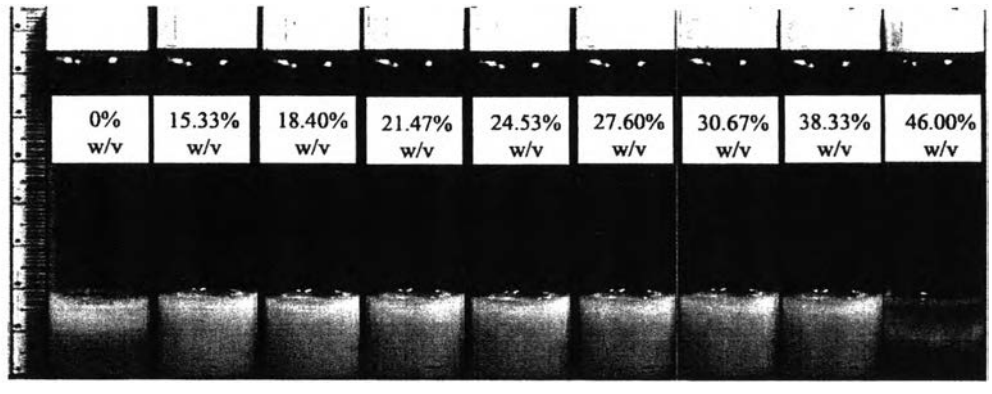

Figure 4.2 Photograph of the emulsion stability after 24 hrs of 18.9% w/v Pluronic f68 that use as surfactant and 4% w/v silk at different concentration of coconut oil.

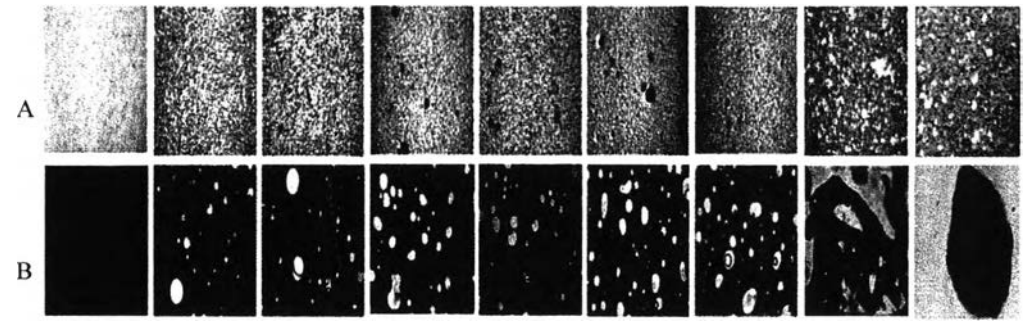

0% (w/v)	15.33% (w/v)	18.4% (w/v)	21.47% (w/v)	24.53% (w/v)	27.60% (w/v)	30.67% (w/v)	38.33% (w/v)	46.00% (w/v)

Figure 4.3 Optical micrographs of the emulsions at different concentrations of oil in water (A) The emulsions are stained with oil soluble dye (Sudan III) (B) The emulsion that are stained with water soluble dye (Phenol red).

4.1.3 The influence of concentration of silk fibroin on the emulsion stability

Figure 4.4 shows a photograph of the emulsions after storage at room temperature (25 °C) for 24 hrs of 18.9% w/v Pluronic f68 and 15.33% w/v coconut oil at different concentration of silk fibroin in total of the emulsion solution at solution volume ratio of Pluronic f68, silk fibroin and Coconut oil is 3:2:1 respectively. The photograph shows that at the emulsions containing 2% w/v silk fibroin separated into an opaque cream layer on the top and a highly turbid emulsion layer at the bottom. At higher concentration of silk fibroin, there was complete the emulsion layer and increasing concentration of silk fibroin did not influenced to emulsion stability. Observation of the emulsion that are stained with oil soluble dye (Sudan III)(Fig4.4A) and water soluble dye (Phenol red)(Fig4.4B) to confirm the emulsion is oil in water emulsion indicate that the emulsions containing 4%-10% w/v silk fibroin are oil in water emulsion.

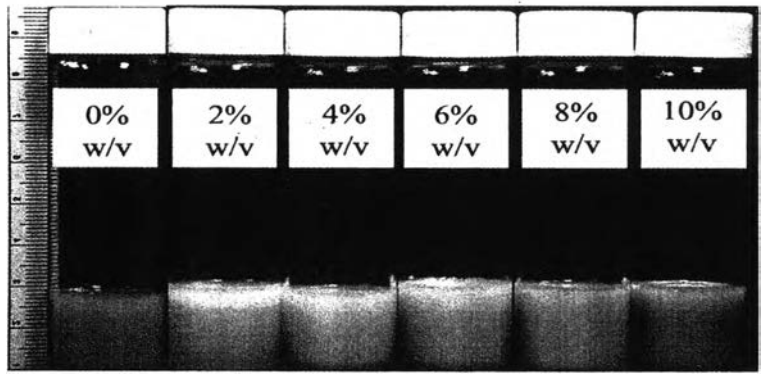

Figure 4.4 Photograph of the emulsion stability of the emulsion containing 18.9% w/v Pluronic f68 that use as surfactant and 15.33% w/v coconut oil at different concentration of silk fibroin after 24 hrs.

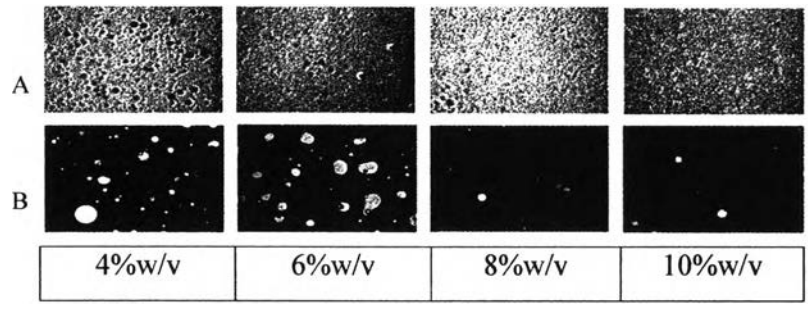

Figure 4.5 Optical micrographs of the emulsions at different concentrations of silk (A) The emulsions were stained with oil soluble dye(SudanIII), (B) The emulsion that were stained with water soluble dye (Phenol red).

4.2 Fabrication of emulsion sheets

4.1.1 Freeze drying method

The coconut oil in silk solution emulsion can form three-dimensional coconut oil incorporated silk fibroin sponge as well as silk fibroin sponge by freeze-drying method(Fig4.6A and B).

Figure 4.6 Photographs of the sponges from freeze drying method (A) the oil incorporated silk fibroin sponge (B) the silk fibroin sponge.

After post treatment with methanol, the structure of coconut oil incorporated silk fibroin sponge changed from random coil to β-sheet that is water insoluble. However, it was high shrinkage because the structure of coconut oil incorporated silk fibroin sponge had high porosity. Moreover, methanol is oil solvent that can dissolve oil from the sponge that affect to highly discharge coconut oil from

the sponge. So, this method was not appropriate for processing the emulsions as a novel material for wound dressing application.

4.2.2 Vacuum drying method

The coconut oil in silk solution emulsion can form three-dimensional coconut oil-incorporated silk fibroin sheet by vacuum drying method(Fig4.7A).After post treatment with methanol, the coconut oil incorporated silk fibroin sheet changed its structure from random coil to β-sheet with a slight shrinkage because the sheet had low porosity. So, coconut oil is low discharged from the sheet. This result indicate that vacuum drying method appropriate for processing emulsion sheet as a novel material for wound dressing application rather than emulsion sponge from freeze drying method.

Figure 4.7 Photographs of the oil incorporated silk fibroin sheets from vacuum drying method.

4.3 Morphology of oil-incorporated silk fibroin sheet

4.3.1 Cross-section and Surface Morphology of uncoated oil-incorporated silk fibroin sheet

SEM micrograph of the fracture cross-section and surface of methanol-treated oil-incorporated silk fibroin sheets that were fabricated by using vacuum air-drying after removing oil. The morphology of methanol-treated oil-incorporated silk fibroin sheets was observed at various concentrations of coconut oil (w/v) in homogeneous solution of 18.9% w/v Pluronic f68 and 10% w/v silk fibroin. The fracture surface and cross-section of methanol-treated oil-incorporated silk fibroin sheets after removing oil were observed at magnification of 150 (see Figure 4.8 and 4.9 respectively) and 3500 (see Figure 4.10 and 4.11 respectively). The morphology observation of the methanol-treated silk fibroin blend sheets after immersed in

chloroform, ethanol and water was done at magnification 150 (see Figure 4.8). The surface of methanol-treated silk fibroin/Pluronic f68 sheet without coconut oil exhibited smoother surface with slightly cracking than methanol-treated silk fibroin/Pluronic f68 sheet with coconut oil because of more homogeneous blending of silk fibroin and Pluronic f68. The cracks on surface of methanol-treated silk fibroin/Pluronic f68 sheet with coconut oil that caused by extracting oil by using chloroform and dehydration by using ethanol, The cracks on the surface decreased when the oil increased and the surface was smoother at 15.33 %w/v coconut oil. This result indicates that miscible blend of the methanol-treated oil-incorporated silk fibroin sheets can be achieved at 15.33% w/v Coconut oil, 18.9% w/v Pluronic f68 and 10 % w/v silk in total mixture solution volume, the solution volume ratio of Pluronic f68, silk fibroin and Coconut oil was 3:2:1 respectively. This observation was clearly seen at magnification of 3500 (see Figure 4.10) confirming that the methanol-treated oil-incorporated silk fibroin sheets at 15.33% w/v coconut oil had smooth surface with low porosity for controlling release of oil into wound and absorbing exudates from wound.

Interestingly, after removing oil by chloroform extraction, the fractured cross-section of the methanol-treated oil-incorporated silk fibroin sheets was observed at magnification of 150 (see Figure 4.10). In Figure 4.10 (A), the globular structure of silk fibroin connect together indicating miscible blend of 10% w/v silk fibroin and 18.9% w/v Pluronic f68 in total solution volume. This observation was clearly seen at magnification of 3500 as shown in Figure 4.12 (A) exhibiting that aggregated Pluronic f68 on spherical shape of silk fibroin connected together, and larger gaps occurred between each globular unit. At this point, the model of the formation of micellar structure of silk fibroin via self assembly was proposed to clearly explain globular shape of silk fibroin as shown in Figure 4.8. For methanol-treated silk fibroin/Pluronic f68 blend sheet with coconut oil at the same solution volume ratio of silk fibroin and Pluronic f68 at various concentrations of coconut oil, the structure was porous. Size of pores was decreased by increasing concentration of coconut oil (See Figure 4.12 (B), 4.12 (C), 4.12 (D), 4.12 (E), 4.12 (F)). In Figure 4.12 (F) shows the miscible blend of 15.33% Coconut oil in 10% w/v silk fibroin and 18.9% pluronic f68 at the same solution volume ratio. However, the globular

structure was irregular because microcellular formation of fibroin proteins were disturbed by interaction of coconut oil with hydrophobic block of silk fibroin.

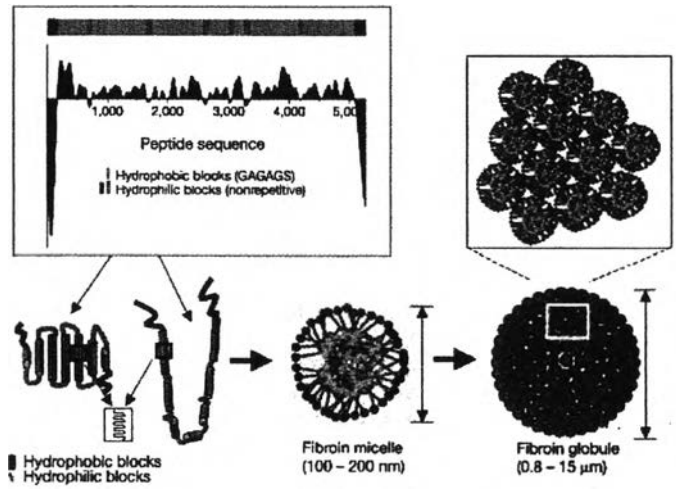

Figure 4.8 Formation of micellar structure of silk fibroin via self assembly.

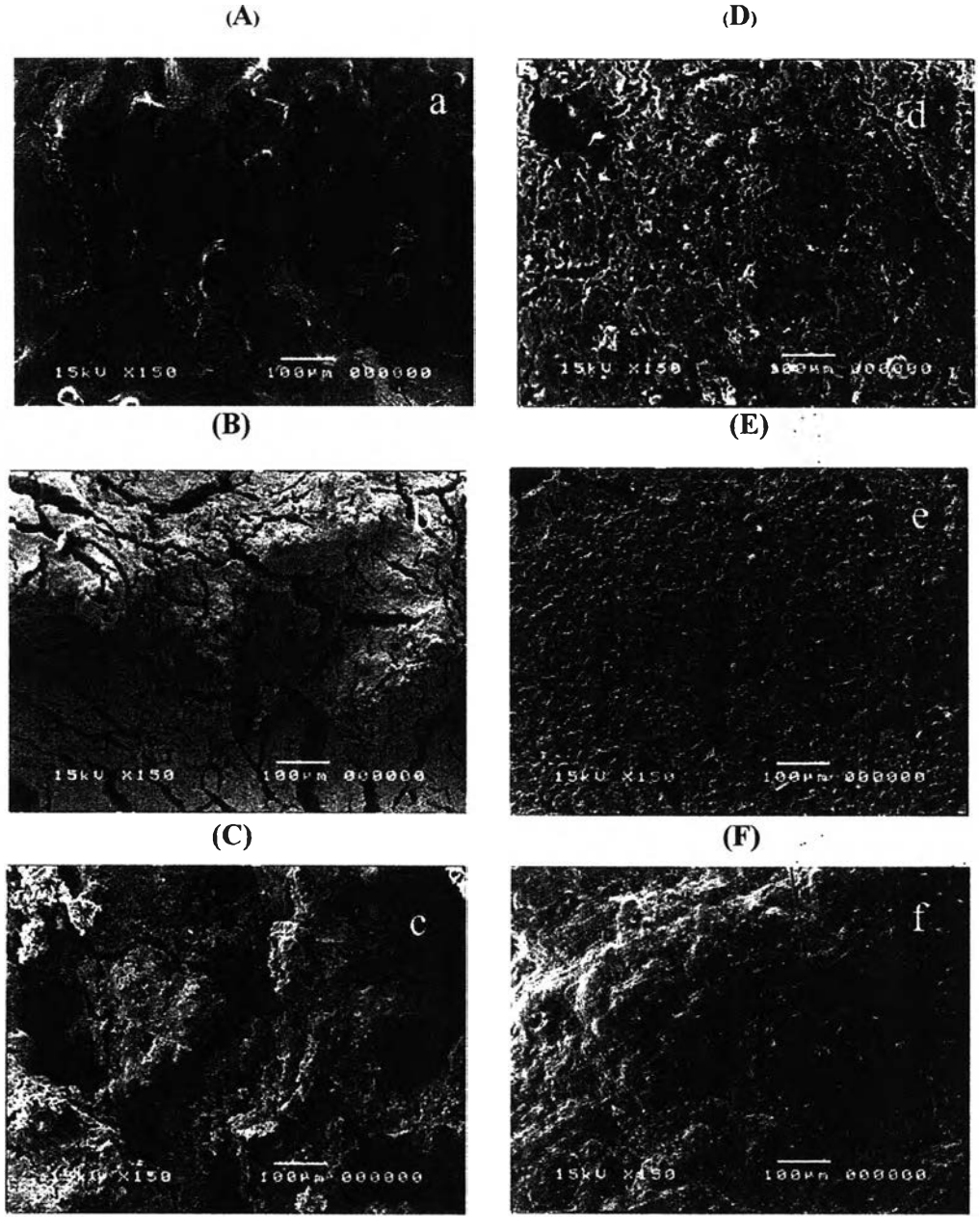

Figure 4.9 SEM images of surface of (A) 0% w/v coconut oil, (B) 1.53% w/v coconut oil, (C) 4.60% w/v coconut oil, (D) 7.67% w/v coconut oil, (E) 10.73% w/v coconut oil, (F) 15.33% w/v coconut oil, incorporated silk fibroin sheet of 18.9% w/v Pluronic f68 and 10% w/v Silk fibroin at different concentration of coconut oil in total volume of emulsion solution after removing oil by using chloroform and dehydration with ethanol at a magnification of 150.

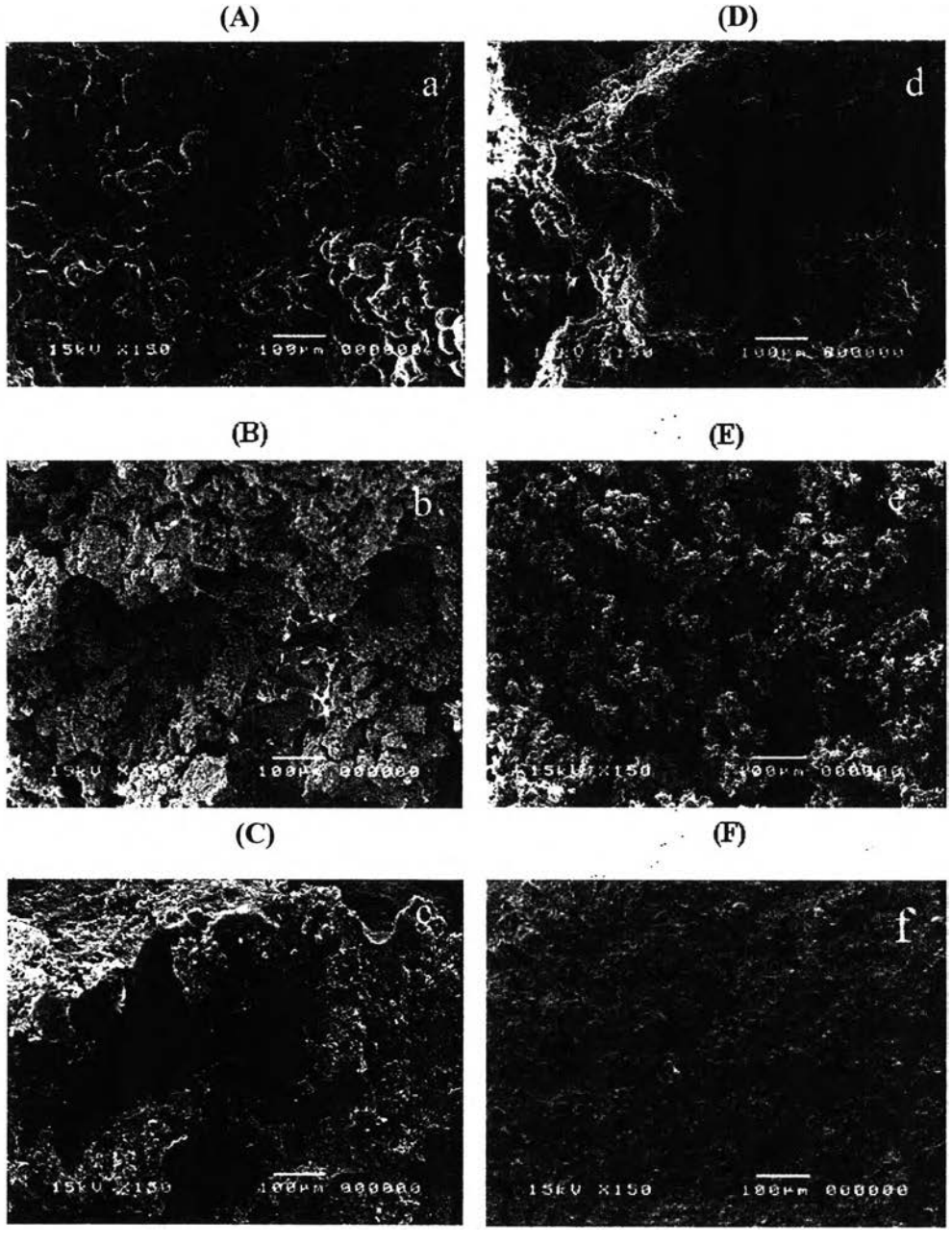

Figure 4.10 SEM images of Cross section (A) 0% w/v coconut oil, (B) 1.53% w/v coconut oil, (C) 4.60% w/v coconut oil, (D) 7.67% w/v coconut oil, (E) 10.73% w/v coconut oil, (F) 15.33% w/v coconut oil, incorporated silk fibroin sheet of 18.9% w/v Pluronic f68 and 10% w/v Silk fibroin at different concentration of coconut oil in total volume of emulsion solution after remove oil by using chloroform and dehydration with ethanol at a magnification of 150.

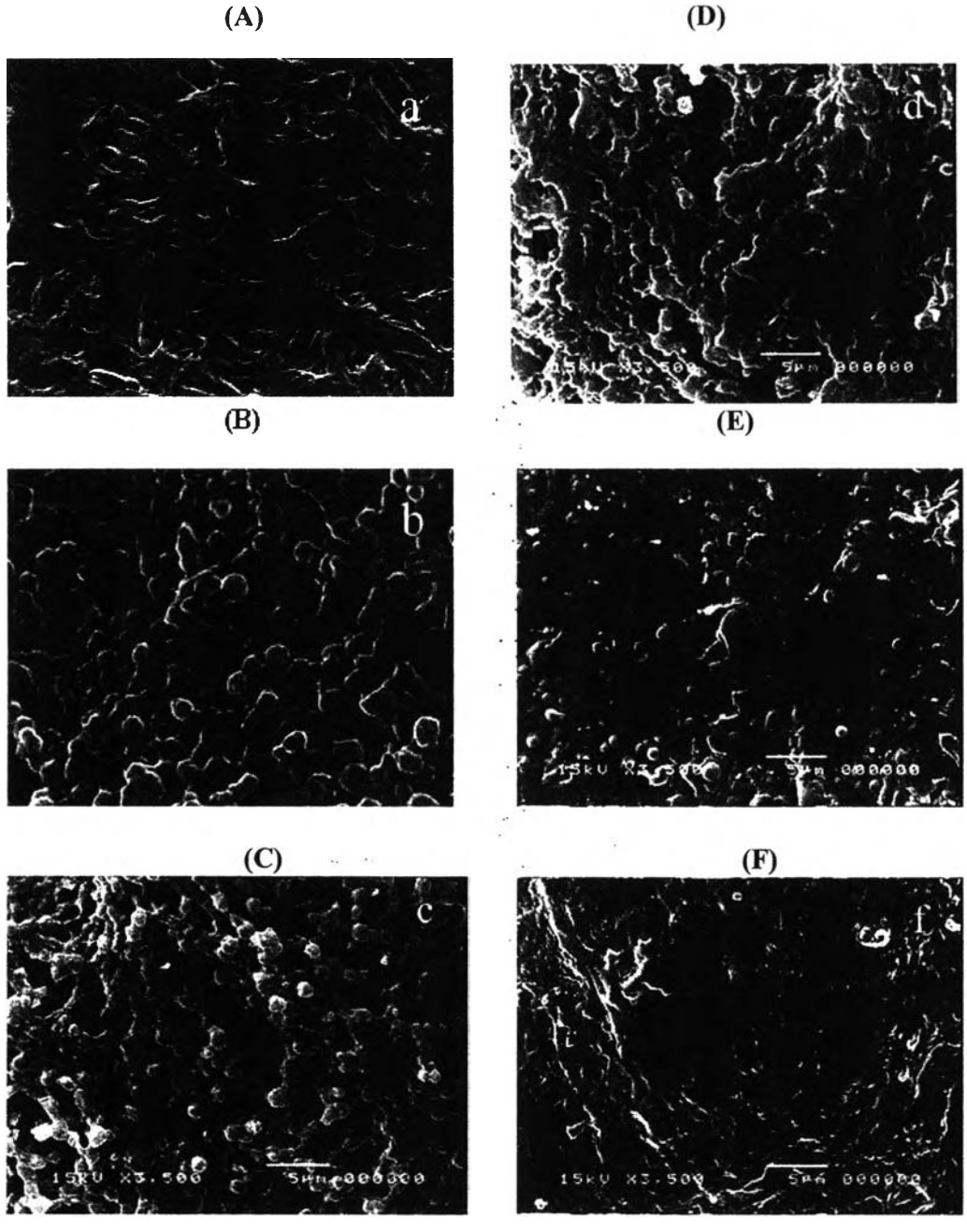

Figure 4.11 SEM images of surface (A) 0% w/v coconut oil, (B) 1.53% w/v coconut oil, (C) 4.60% w/v coconut oil, (D) 7.67% w/v coconut oil, (E) 10.73% w/v coconut oil, (F) 15.33% w/v coconut oil, incorporated silk fibroin sheet of 18.9% w/v Pluronic f68 and 10% w/v Silk fibroin at different concentration of coconut oil in total volume of emulsion solution after remove oil by using chloroform and dehydration with ethanol at a magnification of 3500.

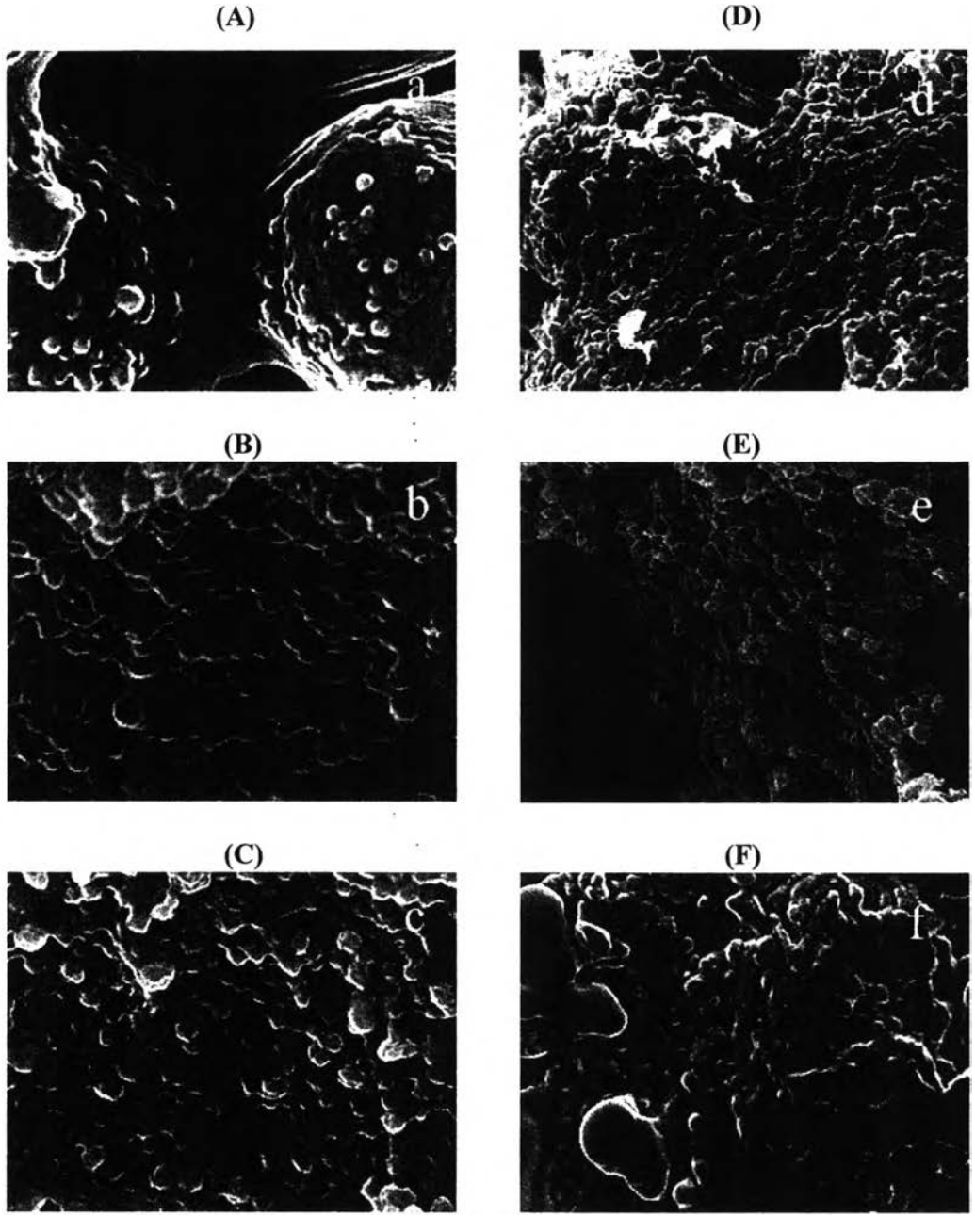

Figure 4.12 SEM images of Cross section of (A) 0% w/v coconut oil, (B) 1.53% w/v coconut oil, (C) 4.60% w/v coconut oil, (D) 7.67% w/v coconut oil, (E) 10.73% w/v coconut oil, (F) 15.33% w/v coconut oil, incorporated silk fibroin sheet of 18.9% w/v Pluronic f68 and 10% w/v Silk fibroin in total volume of emulsion solution after remove oil by using chloroform and dehydration with ethanol at a magnification of 3500.

4.3.2 Morphology of oil-incorporated silk fibroin sheet coated with methanol-treated silk fibroin

SEM images of the surface and cross-section morphology of oil-incorporated silk fibroin sheet coated with methanol-treated silk fibroin are shown in Figure 4.13. These micrographs were obtained to observe the morphology of coated surface of the oil-incorporated silk fibroin sheet with methanol-treated silk fibroin film that was important to control release of oil.

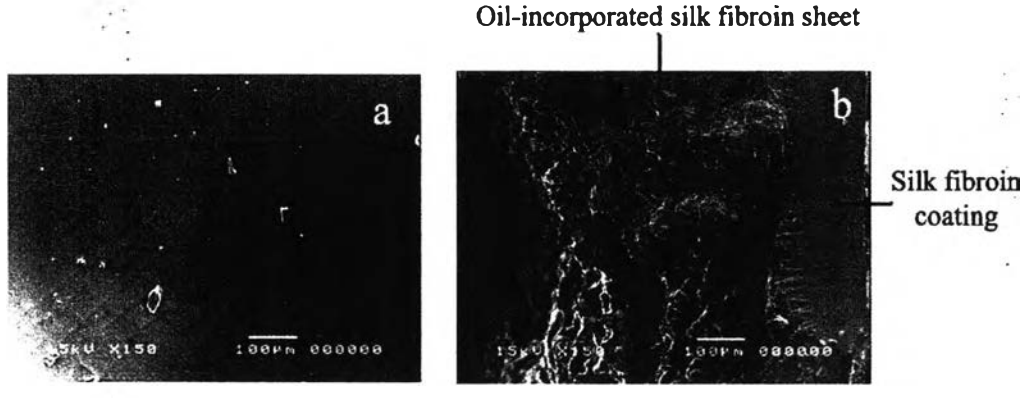

Figure 4.13 SEM images of the oil-incorporated silk fibroin sheet coated with methanol-treated silk fibroin film (a) the surface morphology (b) the cross-section morphology at a magnification of 150.

4.4. Characterization of oil-incorporated silk fibroin sheets

4.4.1 Chemical structure of oil-incorporated silk fibroin sheet

The FT-IR spectra of the silk fibroin, Coconut oil, Pluronic f68 and the oil-incorporated silk fibroin sheet after methanol treatment were shown in Figure 4.14. Figure 4.14 (a) illustates FT-IR spectra of the silk fibroin before methanol treatment, exhibite the characteristic absorption peaks of amide I (C=O stretching) at 1639 cm^{-1}, amide II (N–H deformation) at 1540 cm^{-1}, and amide III (C–N stretching) at 1240 cm^{-1}. These peaks are in good agreement of the random coil fibroin (Yamada et al., 2003). After the oil-incorporated silk fibroin sheet was treated with methanol, the peaks of amide I and amide II were shifted to 1626 and 1529 cm^{-1}, respective and

the strong absorption band at 1244 cm^{-1} in the amide III band was observed (Tsuboi et al., 2001). The new absorption shoulder observed at 1701 and 1281 cm^{-1} in Figure 4.14 (e) are the characteristic absorptions of β-sheet form of silk fibroin (Yamada et al., 2003). For Pluronic f68, the FT-IR spectra exhibited the characteristic absorption peaks of Pluronic f68 presenting at 951 cm^{-1} (C-O sym-metrical structure for Pluronic F68),1113 cm^{-1} (C-O asymmetrical stretching vibrations for Pluronic F68), methylene (CH_2 deformation) at 1471 cm^{-1} and methyl (CH stretching in C-CH_3) at 2876 cm^{-1} and hydroxyl (–OH stretching band) at 3649 cm^{-1}as shown in Figure 4.14 (b). For coconut oil, the FT-IR spectra shown in Figure 4.14 (c) exhibited the characteristic absorption peaks of fatty acid, being presented ester group (C=O stretching) at 1747 cm^{-1}, methylene (CH_2 deformation) at 2854 cm^{-1} and methyl (CH stretching in C-CH_3) at 2925 cm^{-1} and phenolic compounds were exhibited absorption band of methylene (CH_2 deformation) at 2854 cm^{-1}, methyl (CH stretching in C-CH_3) at 2925 cm^{-1}, phenyl skeletal at 1466 cm^{-1}, methyl symmetric bending at 1378 cm^{-1} and plane bending of phenyl at 1162 cm^{-1} (Nakanishi et al., 1977).

Considering Figure 4.14 (d) for the FT-IR spectra of the oil-incorporated silk fibroin sheet before treated with vapor methanol, it shows an obvious characteristic absorbtion peaks of silk fibroin at 1639 cm^{-1}, 1540 cm^{-1} and 1240 cm^{-1}, Pluronic f68 at 1113 $cm^{-1}$and 951 cm^{-1} and coconut oil at 1747 cm^{-1}, 2854 cm^{-1} and 2925 cm^{-1}. After treated with vapor methanol, the FT-IR spectra shows the characteristic absorbtion peaks of β-sheet form of silk fibroin in at 1626 cm^{-1},1529 cm^{-1}, 1234 cm^{-1} and the new absorption shoulder at 1701 and 1281 cm^{-1}(see Figure 4.15 (e)). These absorbtion peak confirmed that the structure of oil-incorporated silk fibroin sheet was changed from random coil to β-sheet after vapor methanol treatment and indicated that Pluronic f68 and Coconut oil were remained in it.

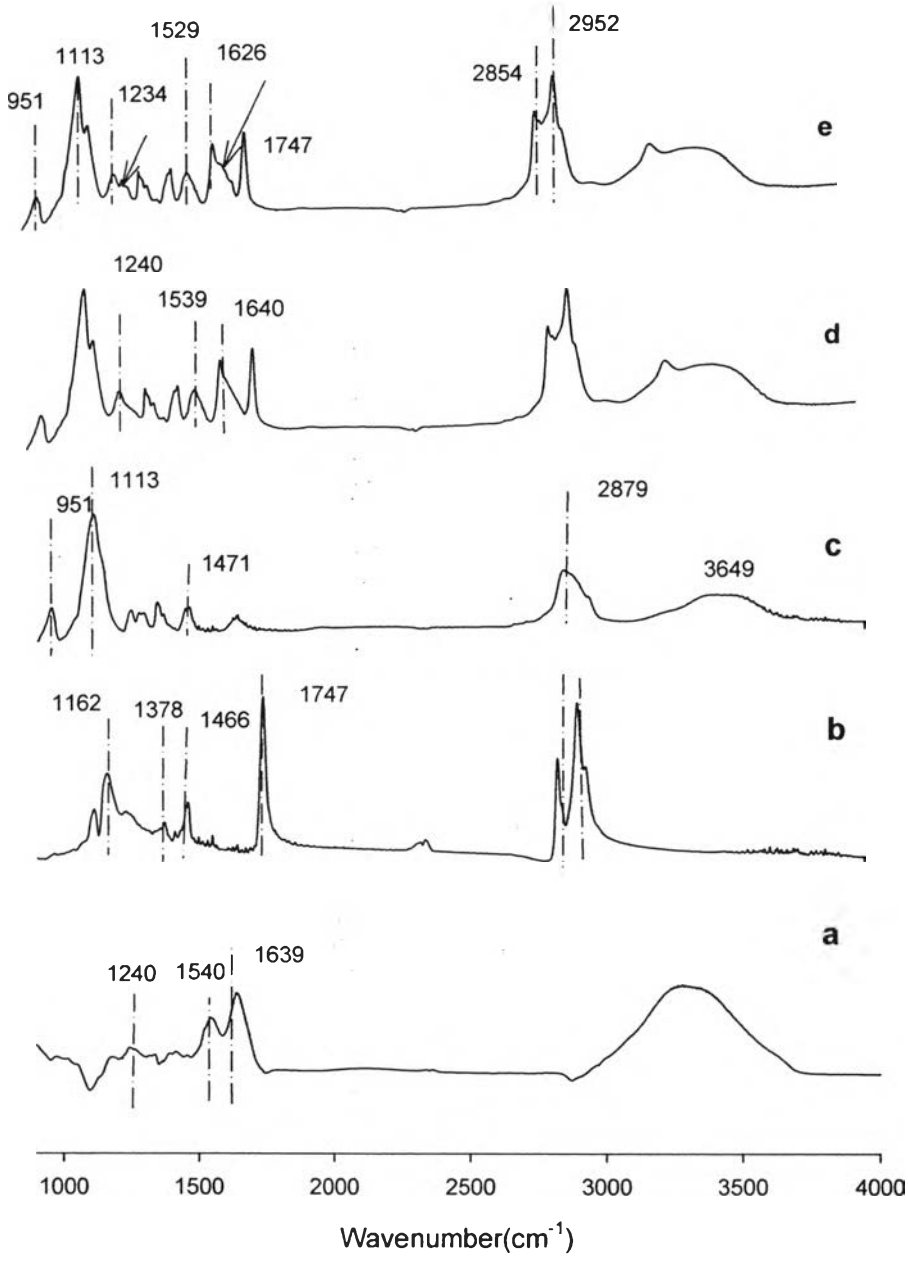

Figure 4.14 FT-IR spectra of the silk fibroin (a), Coconut oil (b), Pluronic f68 (c), the oil-incorporated silk fibroin before vapor methanol treatment (d) and the oil-incorporated silk fibroin after vapor methanol treatment (e). Arrows indicate the absorption shoulder.

4.4.2 Thermal Analysis

Thermogravimetric analysis (TGA) was carried out to confirm the composition of the oil-incorporated silk fibroin sheet and to investigate the thermal stability of silk fibroin, Pluronic f68, coconut oil and the oil-incorporated silk fibroin sheet. The results are shown in Figure 4.15. The weight loss of the silk fibroin sheet at around 100 °C could be due to loss of moisture. The silk fibroin sheet began to significantly lose in the weight near 240 °C and the weight residue further declined at a lower rate at around 330 °C. This is in agreement with the result reported by Lee et al. (2005) where the thermal decomposition was observed at 250 and 309 °C. Zhang et al. (2002) reported that a large substantial weight loss of the *Bombyx mori* silk fibroin film at around 280 °C was ascribed to the thermal decomposition of silk fibroin film and further weight loss taking place from 320 to 500 °C at a lower rate could also be observed. In the case of Pluronic f68 and coconut oil, the initial weight loss was observed at 320 and 257 °C, respectively and both of them decomposed immediately in a single continuous step.

The DTG curve for thermal decomposition of the oil-incorporated silk fibroin sheet in Figure 4.16 took place in three distinct steps. The first step represents decomposition of silk fibroin at around 280 °C. The second step, between 300 and 400 °C, represents decomposition of pluronic f68 that is confirmed by the TGA curve of silk/pluronic f68 and the third step represents decomposition of residue weight of coconut oil at around 550 °C. The results confirm that, all constituents remained in the oil-incorporated silk fibroin sheet after the methanol treatment.

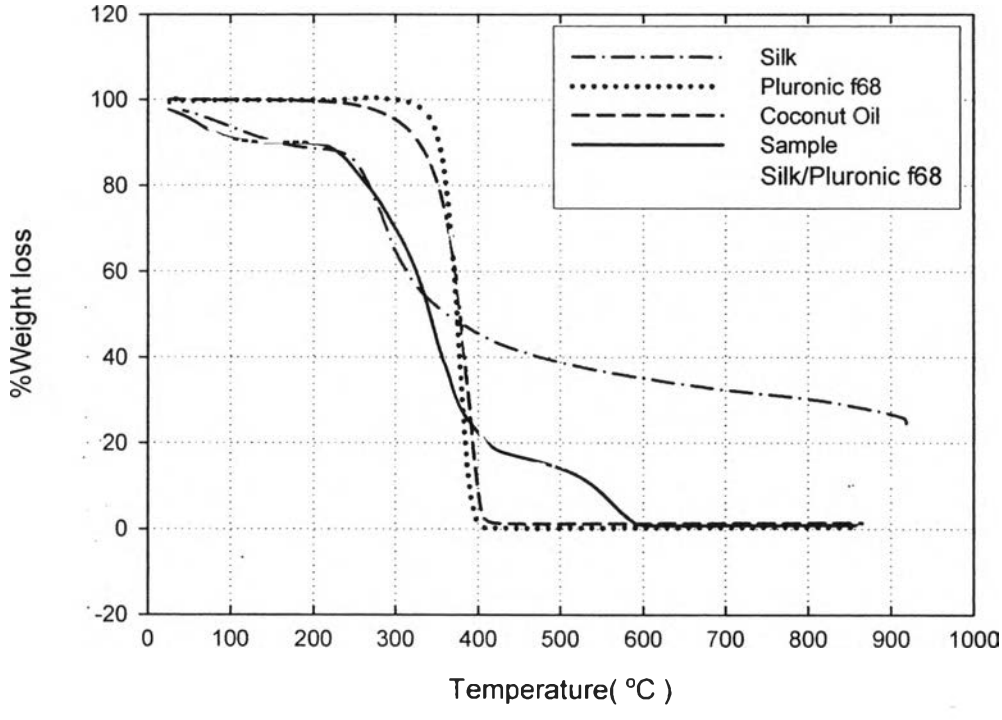

Figure 4.15 Thermogravimetric analysis of silk fibroin, Pluronic f68, coconut oil, sample of the oil-incorporated silk fibroin sheet after methanol treatment and silk fibroin/Pluronic f68.

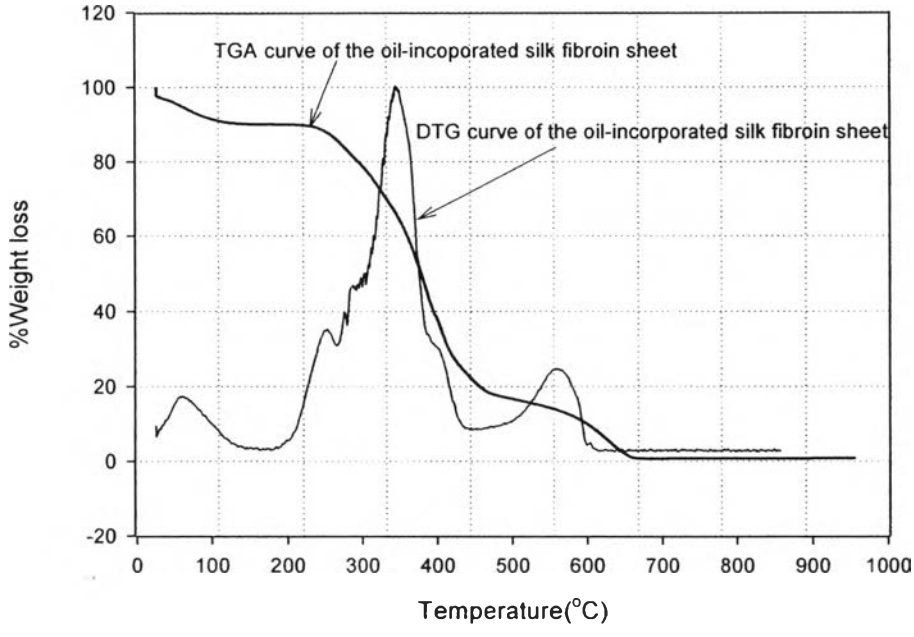

Figure 4.16 TGA and DTG curves of the oil-incorporated silk fibroin sheet under nitrogen environments.

4.5 Releasing Behavior

The release profile of coconut oil from uncoated and methanol- treated silk fibroin with single, double and triple-coating of the oil-incorporated silk fibroin sheets under skin condition (37°C, PH 5.5) are shown in Figure 4.17. Multiple coating was made to change the thickness of the coating on the oil-incorporated silk fibroin sheets in order to observe the effective of coating thickness on the release profile of coconut oil. The release profiles of the oil-incorporated silk fibroin sheets coated with silk fibroin film were compared with that of uncoated oil-incorporated silk fibroin sheets. As shown in this figure, sustained release profiles were achieved for three samples coated with methanol-treated silk fibroin film since the methanol-treated silk fibroin film prevented rapid diffusion of the coconut oil. It was observed that resistance to transport of the coconut oil increased with increasing the length of diffusion path, in other words, increasing the number of coatings. The release rate

constants of oil-incorporated silk fibroin sheets coated with methanol-treated silk fibroin film were smaller than the uncoated ones (K=77.62% min^{-1}, R^2=0.97). Release rate constants were found to be 72.44, 66.07, 39.81% $min^{-1}$with the regression coefficient (R^2) value of 0.95, 0.99, 0.98 for the oil-incorporated silk fibroin sheets with single-coating, double-coating, triple-coating respectively. The 50% of oil was released from uncoated tablet within 288 min (t_{50}=288 min). The t_{50} values were determined to be 312, 330, and 870 min for single-coated, double-coated and triple-coated oil-incorporated silk fibroin sheets, respectively. The release rate of coconut oil from coated oil-incorporated silk fibroin sheets was significantly decreased due to more barrier hindrance to transport of oil increased with increasing the length of diffusion path by thicker coating materials. The decrease in release rate with increasing number of coating was as expected result. So, thickness is an important factor to oil releasing behavior of the oil-incorporated silk fibroin sheets. From this releasing profile, the release rate of triple-coated sheets was observed with high constant rate and became to be constant at long time but the oil was released only 88% of total oil in the oil- incorporated silk fibroin sheets. While the double-coated oil-incorporated silk fibroin sheets with methanol-treated silk fibroin film could release oil up to 95% of total oil with comparable releasing profile.

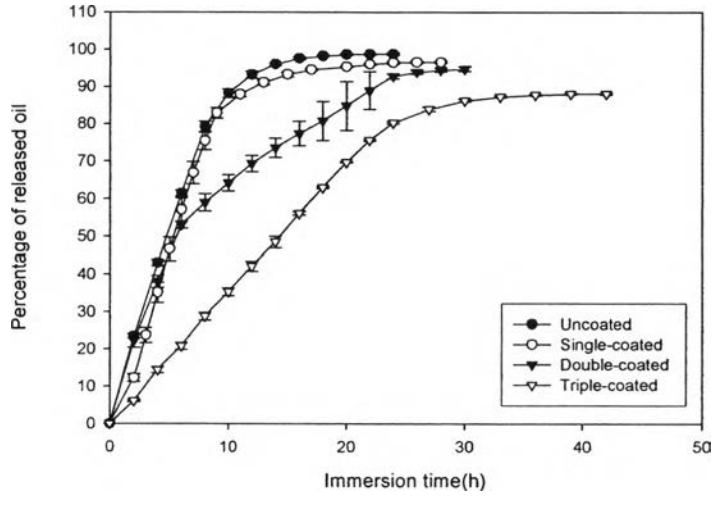

Figure 4.17 Influence of coating thickness on the release profile of the oil-incorporated silk fibroin sheet coated with methanol-treated silk fibroin film.

4.6 Degree of Swelling and Equilibrium Fluid Content

In this work, the degree of swelling and equilibrium fluid content under skin condition (37°C, pH 5.5), were measured. These characteristics indicated the absorption abilities of wound dressing that was important for quick absorption of exudates. The effect on degree of swelling and equilibrium water content of methanol-treated silk fibroin film coating on the oil-incorporated silk fibroin sheets show in Figure 4.18 and Figure 4.19 respectively. For uncoated oil-incorporated silk fibroin sheets, degree of swelling and equilibrium water content are rapidly increased in short time and dropped to lower than initial mass because of disintegration of uncoated oil-incorporated silk fibroin sheets. For single-coated sheet, the degree of swelling and equilibrium fluid content increased with time until saturated point at 15 hr and after that the degree of swelling decreased due to high diffusion of oil from the sheet to the buffer solution. This problem was not observed in double-coated and triple-coated sheets because the number of layer of the coated methanol-treated silk fibroin film was enough to sustain oil in the oil-incorporated silk fibroin sheet. The double-coated sheet had higher degree of swelling and equilibrium fluid content than the triple-coated sheet because more barrier hindrance to transport of water increased with increasing the length of diffusion path by thicker coating methanol-treated silk fibroin films. The water absorption of the oil-incorporated silk fibroin sheets was caused by both chemical and physical structure; for chemical structure, protein fibroin in silk has more hydrophilic in light chain fibroin (Kaplan et al., 1998) that is expected to absorb molecule of water; for physical structure, the oil-incorporated silk fibroin sheet is three-dimensional porous structure maintained by vacuum air-drying method. These observations indicate that the oil-incorporated silk fibroin sheet has absorption ability that can be used to control wound exudates and keep moist environment on the wound.

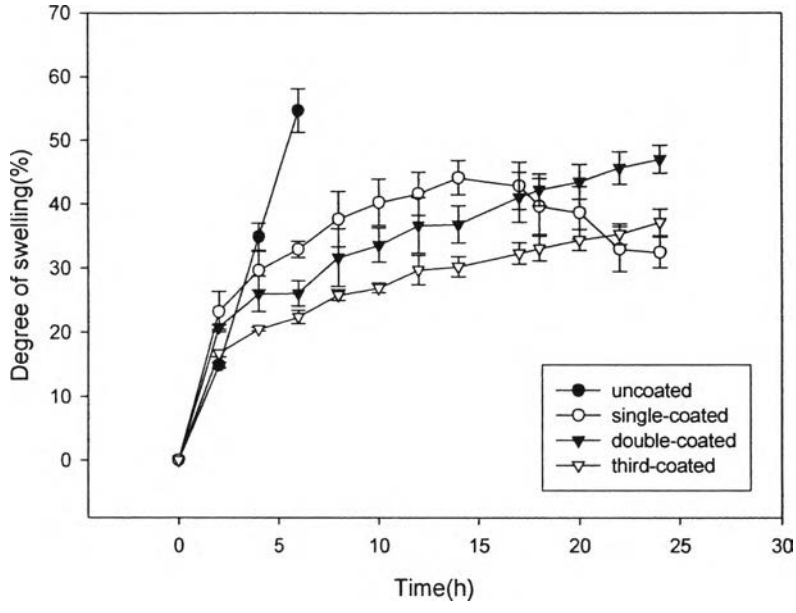

Figure 4.18 Degree of swelling of the oil-incorporated silk fibroin sheet coated with methanol-treated silk fibroin film under skin condition (37°C, pH 5.5).

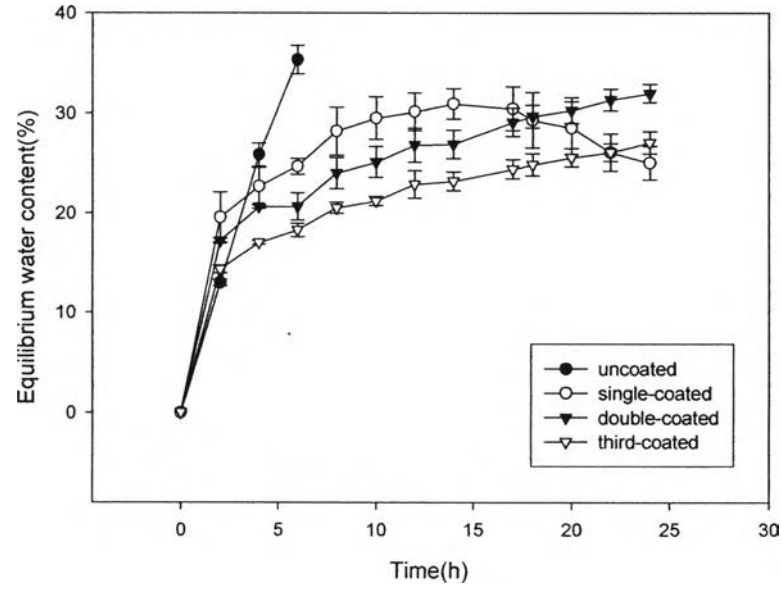

Figure 4.19 Equilibrium water content (%) of the oil-incorporated silk fibroin sheet coated with methanol-treated silk fibroin film under skin condition (37°C, pH 5.5).

4.7 Evaporative water loss

The water loss from oil-incorporated silk fibroin sheet coated with methanol-treated silk fibroin film on exposure to the air was evaluated to examine its behavior when was used as a dressing over a dry wound. As shown in Figure 4.20, the loss of water after 2 h was approximately 20% for single-coated sheet and 10% for double-coated and triple-coated sheets and within 10 h, the loss of water became constant. It is clear from the assessment of evaporative water loss that the material will lose its water content when exposes to air under dry conditions during short periods. Therefore, these dressings may be more beneficial to wounds with more exudates in early-stage wound.

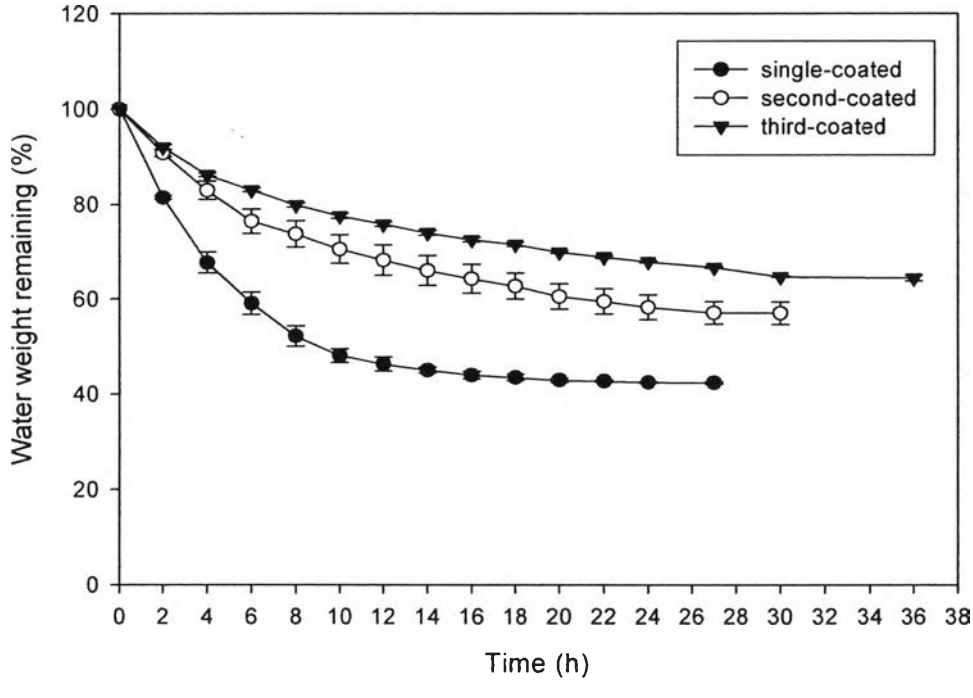

Figure 4.20 Evaporative water loss from the oil-incorporated silk fibroin sheets coated with methanol-treated silk fibroin film under skin condition (37°C).

4.7 Weight loss

The percentage weight loss of the methanol-treated oil-incorporated silk fibroin sheets after incubation in acetate buffer solution (pH 5.5) is shown in figure 4.21. Increased percentage weight loss is observed with time. The weight loss of the oil-incorporated silk fibroin sheets was observed approximately 28 % of initial weight. This study indicates that after vapor methanol treatment, the structure of oil-incorporated silk fibroin sheet was changed from random coil to β-sheet only the surface but in bulk of the oil-incorporated silk fibroin sheet, the structure remained random coil structure.

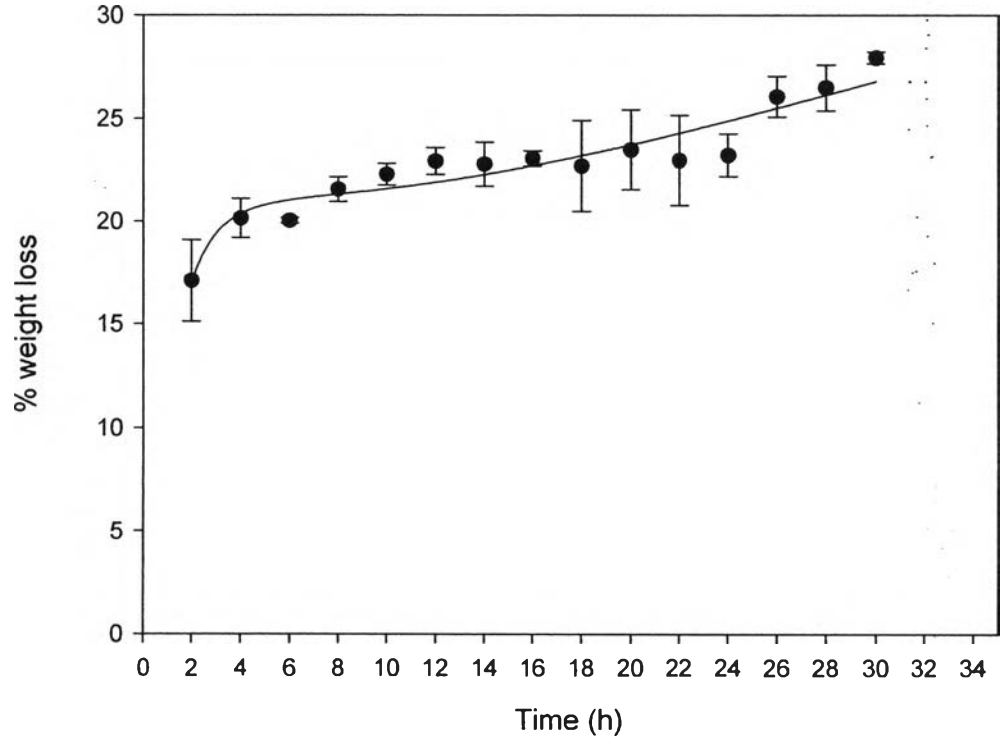

Figure 4.21 Percentage weight loss of the methanol-treated oil-incorporated silk fibroin under skin condition (37°C, pH 5.5).

4.8 Antimicrobial Activity

Antimicrobial activities of 15.33%w/v (in total emulsion solution)of coconut oil-incorporated silk fibroin sheets were investigated against 10^{-6} colony units per ml (cfu/ml) of Escherichia coli (Table 4.1) and Staphylococcus aureus (Table 4.2). The 15.33%w/v (in total emulsion solution) of coconut oil -incorporated silk fibroin sheets was observed to be 97.63% and 99% reduction in viable E. coli and S. aureus, respectively because lauric acid in coconut oil had antimicrobial activity(Dawson et al., 2002).Not only lauric acid in coconut oil that had antimicrobial activity but also 18.9% w/v Pluronic f68 that is slightly against E. coli and S. aureus since extensive Pluronic f68 is extensively used as a wound cleanser in humans without discernable side effects that cause non-favor condition for colonization of bacteria. For pure silk fibroin, there was no reduction in viable counts; on the contrary, there was a 1.86% and 0.12% increase in the viable counts of E. coli and S. aureus, respectively. The bacteria reduction was clearly observed in figure 4.22 demonstrating that the oil-incorporated silk fibroin sheets had good antimicrobial activity for both E. coli (Gram-negative) and S. aureus (Gram-positive). The antibacterial activity against E. coli was lower than that against S. aureus, probably due to the difference in cell walls between Gram-positive and Gram-negative bacteria. The cell wall of the Gram-negative consists of lipids, proteins and lipo-polysaccharides (LPS) that provide effective protection against biocides whereas that of the Gram-positive does not consists of LPS (Feng et al., 2000)

Table 4.1 Antimicrobial activity of 15.33%w/v (in total emulsion solution) of coconut oil -incorporated silk fibroin sheets against Staphylococcus aureus

Condition	Control	Silk fibroin	Silk fibroin /Pluronic f68	Silk fibroin/Pluronicf68 /Coconut oil
CFM	276±17.69	280.33±7.57	178.66±17.21	4.67±2.52
BRR (%)	-	-0.12	36.19	99

Table 4.2 Antimicrobial activity of 15.33%w/v (in total emulsion solution) of coconut oil -incorporated silk fibroin sheets against Escherichia coli

Condition	Control	Silk fibroin	Silk fibroin /Pluronic f68	Silk fibroin/Pluronicf68 /Coconut oil
CFM	197±34.12	200.67±38.59	128±21.93	4.67±2.52
BRR (%)	-	-1.86	35.03	97.63

Note: Colony forming (CFM)

Condition	control	Silk fibroin	Silkfibroin/ Pluronic f68	Silk fibroin/ Pluronicf68/ Coconut oil
S. aureus	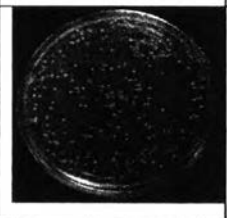	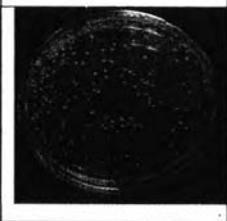	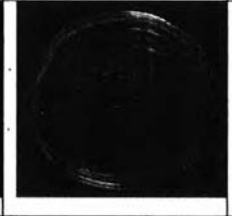	
E. coli	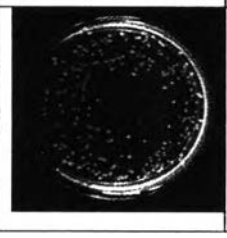	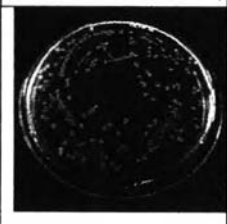	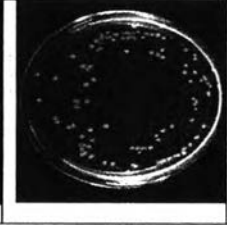	

Figure 4.22 Photographs of the colony forming unit of 15.33%w/v of coconut oil -incorporated silk fibroin sheets against Escherichia coli and Staphylococcus aureus.